
Efficient Algorithms for Finite Horizon and Streaming Restless Multi-Armed Bandit Problems

Aditya Mate¹Arpita Biswas¹Christoph Siebenbrunner¹Milind Tambe¹

¹School of Engineering and Applied Sciences, Harvard University, Cambridge, MA, USA
 aditya_mate@g.harvard.edu, {arpitabiswas, csiebenbrunner}@seas.harvard.edu, milind_tambe@harvard.edu

Abstract

Restless Multi-Armed Bandits (RMABs) have been popularly used to model limited resource allocation problems. Recently, these have been employed for health monitoring and intervention planning problems. However, the existing approaches fail to account for the arrival of new patients and the departure of enrolled patients from a treatment program. To address this challenge, we formulate a *streaming bandit* (S-RMAB) framework, a generalization of RMABs where heterogeneous arms arrive and leave under possibly random streams. We propose a new and scalable approach to computing index-based solutions. We start by proving that index values decrease for short residual lifetimes, a phenomenon that we call index decay. We then provide algorithms designed to capture index decay without having to solve the costly finite horizon problem, thereby lowering the computational complexity compared to existing methods. We evaluate our approach via simulations run on real-world data obtained from a tuberculosis intervention planning task as well as multiple other synthetic domains. Our algorithms achieve an over $150\times$ speed-up over existing methods in these tasks without loss in performance. These findings are robust across multiple domains.

1 INTRODUCTION

In community healthcare settings, adherence of patients to prescribed health programs, that may involve taking regular medication or periodic health checkups, is critical to their well-being. One way to improve patients' health outcomes is by tracking their health or monitoring their adherence to such programs and designing intervention schemes to help patients alleviate health issues such as diabetes [Newman

et al., 2018], hypertension [Brownstein et al., 2007], tuberculosis [Chang et al., 2013, Rahedi Ong'ang'o et al., 2014], depression [Löwe et al., 2004, Mundorf et al., 2018], etc. However, health interventions often require dedicated time of healthcare workers, which is a severely scarce resource, especially in the global south. Moreover, planning interventions is made more challenging by the fact that the extent of adherence of patients may be both, uncertain as well as transient. Consequently, the healthcare workers have to grapple with this sequential decision making problem of deciding which patients to intervene on, with limited resources, in an uncertain environment. Existing literature on healthcare monitoring and intervention planning (HMIP) [Akbarzadeh and Mahajan, 2019, Mate et al., 2020, Bhattacharya, 2018] casts this as a *restless multi-armed bandit* (RMAB) planning problem. In this setup, the patients are typically represented by the arms of the bandit and the planner must decide which arms to pull (which patients to intervene on) under a limited budget. In addition to healthcare, RMABs have caught traction as solution techniques in a myriad of other domains involving limited resource planning for applications such as anti-poaching patrol planning [Qian et al., 2016], multi-channel communication systems [Liu and Zhao, 2010b], sensor monitoring tasks [Glazebrook et al., 2006], UAV routing [Le Ny et al., 2008] etc. For ease of presentation, we consider the HMIP problem for motivation but our approach is relevant and can be extended to other real-world domains.

A popular approach, known as the Whittle Index policy [Whittle, 1988], has been shown to work very well, especially under an *indexability* assumption. The existing literature on RMABs however, has mainly focused on problems involving an infinite time horizon (i.e., the health programs are assumed to run forever) and, moreover, the results are limited to settings where no new patients (or arms) arrive midway during the health program. A fairly general approach, proposed by Qian et al. [2016] may be applied even when patients arrive asynchronously, but the method is very expensive computationally and becomes cumbersome to run as the number of patients increases. A more recent approach,

such as that proposed by Mate et al. [2020], exploits the structure of the HMIP and is considerably faster but the method relies on the planning horizon being very large. The fast algorithm suffers a severe deterioration in performance when employed on finite horizon settings.

We consider a general class of RMABs, which we call *streaming restless multi-armed bandits*, or S-RMAB. In an S-RMAB instance, the arms of the bandit are allowed to arrive asynchronously, that is, the planner observes an incoming and outgoing stream of bandit arms. The classic RMAB (both with infinite and finite horizon) is a special case of the S-RMAB where all arms appear (leave) at the same time. Additionally, each arm of an S-RMAB is allowed to have its own transition probabilities, capturing the potentially heterogeneous nature of patient cohorts.

Contributions: Towards addressing these challenges, focusing on finite-horizon, we propose a scalable approach for solving the S-RMAB. We start by showing that index values decrease as the residual lifetime of an arm approaches zero. We propose new algorithms that make use of this phenomenon to lower the computational complexity compared to existing solutions. We perform experimental evaluations using real-world data. Our algorithms provide over $150\times$ speed-up compared to existing methods without loss in performance. We perform multiple robustness checks using synthetic data to vary important problem parameters. Our main results are robust across all specifications.

2 RELATED WORK

The RMAB problem was introduced by Whittle [1988]. The paper studied the RMAB problem with the goal of maximizing the average reward in a dynamic programming framework. Whittle formulated a relaxation of the problem and provided a heuristic called *Whittle Index policy*. This policy is optimal when the underlying Markov Decision Processes satisfy indexability, which is computationally intensive to verify. Later, Papadimitriou and Tsitsiklis [1994] established that solving RMAB is PSPACE hard, even when the transition rules are known. Since then, specific classes of RMABs have been studied extensively. Qian et al. [2016] studied the infinite horizon RMAB problem and proposed a binary search based algorithm to find Whittle index policy. However, the algorithm becomes computationally expensive as the number of arms grows. Bhattacharya [2018] models the problem of maximizing health information coverage as an RMAB problem and proposes a hierarchical policy which leverages the structural assumptions of the RMAB model. Akbarzadeh and Mahajan [2019] provide a solution for the class of bandits with “controlled restarts” and state-independent policies, possessing the indexability property. Mate et al. [2020] model a health intervention problem, assuming that the uncertainty about the state collapses when an intervention is provided. They provide an algorithm

called *Threshold Whittle* to compute the Whittle indices for infinite horizon RMAB. There are many other papers that provide Whittle indexability results for different subclasses of Partially Observable Markovian bandits [Glazebrook et al., 2006, Hsu, 2018, Sombabu et al., 2020, Liu and Zhao, 2010a]. However, these papers focus on infinite horizon, whereas we focus on the more challenging setting when there is a fixed finite horizon.

The RMAB problem with finite horizon has been comparatively less studied. Nino-Mora [2011] provided solutions to the one-armed restless bandit problem, where only one arm is activated at each time before a time horizon T . Their solution do not directly extend to the scenario when multiple arms can be pulled at each time step. Hu and Frazier [2017] considered finite horizon multi-armed restless bandits with identically distributed arms. They show that an index based policy based on the Lagrangian relaxation of the RMAB problem, similar to the infinite horizon setting, provides a near-optimal solution. Lee et al. [2019] study the problem of selecting patients for early-stage cancer screening, by formulating it as a very restricted subclass of RMAB. All these works consider that all the arms are available throughout T time steps. Some other works, such as [Meuleau et al., 1998, Hawkins, 2003] also adopt different approaches to decomposing the bandit arms, which may be applicable to finite horizon RMABs. These techniques to solving weakly coupled Markov Decision Processes are more general, but consequently less efficient than the Whittle Index approach in settings where indexability assumption holds.

The S-RMAB problem has been studied in a more restricted setting by Zayas-Caban et al. [2019]. They assume that, at each time step, arms may randomly arrive and depart due to random abandonment. However, the main limitation of their solution is the assumption that all arms have the same state-transition dynamics. This assumption does not hold in most of the real-world instances and thus, in this paper, we consider heterogeneous arms—arms are allowed to have their own transition dynamics. We show empirically that our algorithms performs well even with heterogeneous arms.

Another related category of work studied *sleeping arms* for the *stochastic multi-armed bandits* (SMAB) problem, where the arms are allowed to be absent at any time step (Kanade et al. [2009], Kleinberg et al. [2010], Biswas et al. [2015]). However, the SMAB is different from RMAB because, in the former, when an arm is activated, a reward is drawn from a Bernoulli reward distribution (and not dependent on any state-transition process). Thus, the algorithms and analysis of SMABs do not translate to the RMAB setting.

3 STREAMING BANDITS

The *streaming restless multi-armed bandit* (S-RMAB) problem is a general class of RMAB problem where

a stream of arms arrive over time (both for finite and infinite-horizon problems). Similar to RMAB, at each time step, the decision maker is allowed to take active actions on at most k of the available arms. Each arm i of the S-RMAB is a Partially Observable Markov Decision Process (POMDP)—represented by a 4-tuple $(\mathcal{S}, \mathcal{A}, \mathcal{P}, r)$. $\mathcal{S} = \{0, 1\}$ denotes the state space of the POMDP, representing the “bad” state (say, patient’s not adhering to the health program) and “good” state (patient adhering), respectively. \mathcal{A} is the action space, consisting of two actions $\mathcal{A} = \{a, p\}$ where an action a (or, p), denotes the active (or, passive) action. The state $s \in \mathcal{S}$ of the arm, transitions according to a known transition function, $P_{s,s'}^{a,i}$ if the arm is pulled and according to the known function, $P_{s,s'}^{p,i}$ otherwise. We also assume the transition function to conform to two natural constraints often considered in existing literature [Liu and Zhao, 2010b, Mate et al., 2020]: (i) Interventions should positively impact the likelihood of arms being in the good state, i.e. $P_{01}^a > P_{01}^p$ and $P_{11}^a > P_{11}^p$ and (ii) Arms are more likely to remain in the good state than to switch from the bad state to the good state, i.e. $P_{01}^a > P_{01}^p$ and $P_{11}^a > P_{11}^p$. Though the transitions probabilities are known to the planner, the actual state change is stochastic and is only partially observable—that is, when an arm is pulled, the planner discovers the true state of the arm; however, when the arm is not pulled, uncertainty about the true state persists. Under such uncertainties, it is customary to analyze the POMDP using its equivalent belief state MDP representation instead [Mate et al., 2020]. The state space of this MDP is defined by set of all possible “belief” values that the arm can attain, denoted by \mathcal{B}_i . Each belief state $b \in \mathcal{B}_i$ represents the likelihood of the arm being in state 1 (good state). This likelihood is completely determined by the number of days that have passed since that arm was last pulled and the last observed state of the arm [Liu and Zhao, 2010b]. At each time step t , the planner accrues a state-dependent reward r_t from an active arm i , defined as:

$$r_t(i) = \begin{cases} 0 & \text{if } s_t(i) = 0 \text{ (arm } i \text{ is in the bad state at time } t\text{)} \\ 1 & \text{if } s_t(i) = 1 \text{ (arm } i \text{ is in the good state at time } t\text{)}. \end{cases}$$

The total reward¹ of $R_t = \sum_{i \in [N]} (r_t(i))$ is accrued by the planner at time t , which is the sum of individual rewards obtained from the active arms. The planner’s goal is to maximize her total reward collected, $\bar{R} := \sum_{t \in [T]} R_t$. This reward criterion is motivated by our applications in the healthcare intervention domain: interventions here correspond to reminding patients to adhere to their medication schedules and the good and bad states refer to patients either adhering or not adhering. The goal of the planner is to maximize the expected number of times that all patients in the program adhere to their medication schedules. However, due to the limited budget, the planner is constrained to pull at most k arms per time step. Assuming a set of N arms, the problem thus

boils down to determining a policy, $\pi : \mathcal{B}_1 \times \dots \times \mathcal{B}_N \rightarrow \mathcal{A}^N$ which governs the action to choose on each arm given the belief states of arms, at each time step so as to maximize the total reward accumulated across T time steps. Contrary to previous approaches that typically consider arms to all arrive at the beginning of time and stay forever, in this paper we consider streaming multi-armed bandits—a setting in which arms are allowed to arrive asynchronously and have finite lifetimes. We denote the number of arms arriving and leaving the system at a time step $t \in [T]$ by $X(t)$ and $Y(t)$, respectively. Each arm i arriving the system at time t , is associated with a fixed lifetime L_i (for example, L_i can be used to represent the duration of the health program for a patient, which is known to the planner). The arm consequently leaves the system at time $t + L_i$. Thus, instead of assuming a finite set of N arms throughout the entire time horizon, we assume that the number of arms at any time t is denoted by $N(t)$, and can be computed as $N(t) = \sum_{i=1}^t (X(i) - Y(i))$. Thus, the goal of the planner is to decide, at each time step t , which k arms to pull (out of the $N(t) \gg k$ arms), in order to maximize her total reward,

$$\bar{R} := \sum_{t \in [T]} \sum_{i \in N(t)} r_t(i).$$

4 METHODOLOGY

The dominant paradigm for solving RMAB problems is the Whittle index approach. The central idea of the Whittle approach is to decouple the RMAB arms and then compute indices for each arm that capture the “value” of pulling that arm. The Whittle Index policy then proceeds by pulling the k arms with the largest values of Whittle Index. This greedy approach makes the time complexity linear in the number of arms, as indices can be computed independently for each arm. The computation of the index hinges on the notion of a “passive subsidy” m , which is the amount rewarded to the planner for each arm kept passive, in addition to the usual reward collected from the arm. Whittle Index for an arm is defined as the infimum value of subsidy, m that must be offered to the planner, so that the planner is indifferent between pulling and not pulling the arm. To formalize this notion, consider an arm of the bandit in a belief state b . Its active and passive value functions, when operating under a passive subsidy m , can be written as:

$$V_{m,T}^p(b) = b + m + \beta V_{m,T-1}(b P_{11}^p + (1-b) P_{01}^p) \quad (1)$$

$$V_{m,T}^a(b) = b + \beta b V_{m,T-1}(P_{11}^a) + \beta (1-b) V_{m,T-1}(P_{01}^a) \quad (2)$$

The value function for the belief state b is simply, $V_{m,T}(b) = \max\{V_{m,T}^p(b), V_{m,T}^a(b)\}$. The Whittle Index for the belief state b , with a residual lifetime T is defined as: $\inf_m \{m : V_{m,T}^p(b) = V_{m,T}^a(b)\}$. The Whittle Index approach is guaranteed to be asymptotically optimal when a technical condition called *indexability* holds. Intuitively, indexability requires that if for some passive subsidy m , the optimal action

¹For a natural number N , we use the notation $[N] := \{1, \dots, N\}$.

on an arm is passive, then $\forall m' > m$, the optimal action should still remain passive. Equivalently, indexability can be expressed as: $\frac{\partial}{\partial m} V_{m,T}^p(b) \geq \frac{\partial}{\partial m} V_{m,T}^a(b)$.

4.1 EXISTING ALGORITHMS

Qian et al. [2016] present an algorithm that computes Whittle policy up to arbitrary precision by performing a binary search over the space of passive subsidies m , to find that m which sets exactly k out of the N arms as active. For each value of m , on each arm, the optimal action is determined by solving the resulting 2-state 2-action POMDP, with value function given by Equation 1. While this approach can accommodate finite horizon settings, the algorithm is very slow and cumbersome to run for large number of arms.

Mate et al. [2020] presents an efficient algorithm, called *Threshold Whittle*, that computes the Whittle Index. They theoretically prove the asymptotic optimality of their algorithm when a specific type of policies, called ‘forward threshold policies’ are optimal for any value of passive subsidy, m on the bandit arms. The Threshold Whittle algorithm leverages the threshold optimality structure to compute the Whittle Indices in a closed form, and is several orders-of-magnitude faster than Qian et al. [2016]. However, Threshold Whittle is only designed for infinite horizon settings, and consequently, the performance hinges on the planning horizon being sufficiently large.

4.2 INDEX DECAY FOR FINITE HORIZONS

Because the Threshold Whittle algorithm computes the exact Whittle Index for bandits with infinitely lived arms, we consider this as the limiting case of arms with finite horizon as the horizon diverges. For short horizons we observe a phenomenon that we call *index decay*: index values decrease as the residual lifetime of an arm approaches zero. We formalize this observation in Theorem 1. We proceed by stating one fact and proving one useful Lemma, building up towards the Theorem.

Fact 1 *For two linear functions, $f(x)$ and $g(x)$ of x , such that $f'(x) \geq g'(x)$, whenever $f(x_1) < g(x_1)$ and $f(x_2) = g(x_2)$, the following holds: $x_2 > x_1$.*

Lemma 1 *Consider an arm operating under a passive subsidy m . Assuming an initial belief state b_0 , let $\rho^a(b_0, t)$ and $\rho^p(b_0, t)$ denote the probability of the arm being in the good state at time $t \forall t < T$ when policies $\pi^a(t)$ and $\pi^p(t)$ are adopted respectively, such that $\pi^a(0) = a$, $\pi^p(0) = p$, and $\pi^a(t) = \pi^p(t) \forall t \in \{1, \dots, T\}$. Then,*

$$\rho^a(b_0, t) > \rho^p(b_0, t) \forall t \in \{1, \dots, T\}.$$

Proof. We prove this using induction. For the base case, clearly, for $t = 1$:

$$\rho^a(b_0, 1) = b_0 P_{11}^a + (1 - b_0) P_{01}^a \quad (3)$$

$$> b_0 P_{11}^p + (1 - b_0) P_{01}^p \quad (\because P_{s1}^a > P_{s1}^p) \quad (4)$$

$$= \rho^p(b_0, 1) \quad (5)$$

For the inductive step, we assume $\rho^a(b_0, t) > \rho^p(b_0, t)$ and show that it implies $\rho^a(b_0, t+1) > \rho^p(b_0, t+1)$.

$$\rho^a(b_0, t+1) = \rho^a(b_0, t) P_{11}^{\pi(t)} + (1 - \rho^a(b_0, t)) P_{01}^{\pi(t)} \quad (6)$$

$$= \rho^a(b_0, t) (P_{11}^{\pi(t)} - P_{01}^{\pi(t)}) + P_{01}^{\pi(t)} \quad (7)$$

$$> \rho^p(b_0, t) (P_{11}^{\pi(t)} - P_{01}^{\pi(t)}) + P_{01}^{\pi(t)} \quad (8)$$

$$= \rho^p(b_0, t+1) \quad (9)$$

The inductive hypothesis follows, completing the proof. \square

Theorem 1 (Index Decay) *Let $V_{m,T}^p(b)$ and $V_{m,T}^a(b)$ be the T -step passive and active value functions for a belief state b with passive subsidy m . Let m_T be the value of subsidy m , that satisfies the equation $V_{m,T}^p(b) = V_{m,T}^a(b)$ (i.e. m_T is the Whittle Index for a horizon T). Assuming indexability holds, we show that the Whittle index decays for short horizons: $\forall T > 1: m_T > m_1 > m_0 = 0$.*

Proof. We provide our argument for a more general reward criterion than the total reward introduced in Section 3. Consider a discounted reward criterion with discount factor $\beta \in [0, 1]$ (where $\beta = 1$ corresponds to total reward). m_0 is simply the m that satisfies: $V_{m,0}^p(b) = V_{m,0}^a(b)$ i.e., $b + m = b$, thus $m_0 = 0$. Similarly, m_1 can be solved by equating $V_{m_1,1}^p(b)$ and $V_{m_1,1}^a(b)$ as follows:

$$\implies b + m_1 + \beta (b P_{11}^p + (1 - b) P_{01}^p) = \quad (10)$$

$$b + \beta (b (P_{11}^a) + (1 - b) (P_{01}^a))$$

$$\implies m_1 = \beta (b (P_{11}^a - P_{11}^p) + (1 - b) (P_{01}^a - P_{01}^p)) \quad (11)$$

Using the natural constraints $P_{s1}^a > P_{s1}^p$ for $s \in \{0, 1\}$, we obtain $m_1 > 0$.

Now, to show $m_T > m_1 \forall T > 1$, we first show that $V_{m_1, T}^a(b) > V_{m_1, T}^p(b)$. Combining this with the fact that $V_m(\cdot)$ is a linear function of m and by definition, m_T is a point that satisfies $V_{m_T, T}^p(b) = V_{m_T, T}^a(b)$, we use Fact 1 and set $f = V_{m, T}^p(b)$, $g = V_{m, T}^a(b)$, $x_1 = m_1$ and $x_2 = m_T$ to obtain $m_1 < m_T$, and the claim follows. For completeness, we now show that $V_{m_1, T}^a(b) > V_{m_1, T}^p(b)$.

Starting from an initial belief state b_0 , let $\rho^p(b_0, t)$ be the expected belief for the arm at time t , if the passive action was chosen at $t = 0$ and the optimal policy, $\pi^p(t)$ was adopted for $0 < t < T$. Similarly let $\rho^a(b_0, t)$ be the expected belief at time t , if the active action was chosen at $t = 0$ and the same policy, $\pi^p(t)$ (which may not be optimal now) was

adopted for $0 < t < T$. Then, $\rho^a(b_0, 1) - \rho^p(b_0, 1) = m_1 > 0$ as shown above. Note that if we took actions according to $\pi^p(t)$ for $t \in \{1, \dots, T-1\}$ with active action taken at the 0^{th} time step, the total expected reward so obtained is upper bounded by the active action value function, $V_{m_1, T}^a(b_0)$. Thus,

$$V_{m_1, T}^p(b_0) = b_0 + m_1 + \beta \rho^p(b_0, 1) + \sum_{t=2}^T \beta^t \rho^p(b_0, t) \quad (12)$$

$$+ \left(\sum_{t=1}^T \beta^t m_1 \cdot \mathbb{1}_{\{\pi^p(t)=\text{passive}\}} \right) \\ = b_0 + \beta \rho^a(b_0, 1) + \sum_{t=2}^T \beta^t \rho^p(b_0, t) \quad (13)$$

$$+ \left(\sum_{t=1}^T \beta^t m_1 \cdot \mathbb{1}_{\{\pi^p(t)=\text{passive}\}} \right) \\ < b_0 + \beta \rho^a(b_0, 1) + \sum_{t=2}^T \beta^t \rho^a(b_0, t) \quad (14)$$

$$+ \left(\sum_{t=1}^T \beta^t m_1 \cdot \mathbb{1}_{\{\pi^p(t)=\text{passive}\}} \right) \quad (\text{by Lemma 1}) \\ \leq V_{m_1, T}^a(b_0) \quad (15)$$

□

4.3 PROPOSED ALGORITHMS

The key insight driving the design of our solution is that, by accounting for the index decay phenomenon, we can bypass the need to solve the costly finite horizon problem. We make use of the fact that we can cheaply compute index values for arms with residual lifetime 0 and 1, where the index decay phenomenon occurs, and for infinite horizon bandits. Our proposed solution for computing indices for arbitrary residual lifetime is to use a suitable functional form to interpolate between those three observations. We propose an interpolation template, that can be used to obtain two such algorithms, one using a piece-wise linear function and the other using a logistic function.

Recall that we establish in Theorem 1 that the Whittle Index for arms with a zero residual lifetime, is always zero. Similarly, indices for arms with residual lifetime of 1 are simply the myopic indices, computed as the immediate expected improvement in the belief in the next time step upon choosing the active action as against the passive action, computed as: $\Delta b = (b P_{11}^a + (1-b) P_{01}^a) - (b P_{11}^p + (1-b) P_{01}^p)$.

For the linear interpolation, we assume $\hat{W}(h)$, our estimated Whittle Index, to be a piece-wise-linear function of h (with two pieces), capped at a maximum value of TW , corresponding to $h = \infty$, as given by the Threshold Whittle algorithm. The first piece of the piece-wise-linear $\hat{W}(h)$ must pass through the origin, given that the Whittle Index is 0 when the residual lifetime is 0. The slope is determined by $\hat{W}(h=1)$

Algorithm 1: Interpolation Algorithm Template

- 1: Pre-compute the Threshold Whittle Oracle $\text{TW}(b, P^i) \forall b \in \mathcal{B}_i \forall \text{arms } i \in [N]$, with transition matrix, P^i and set of belief states \mathcal{B}_i .
 - 2: **Input:** $\bar{b}_{N \times 1} \in [0, 1]^N$, $\bar{h}_{N \times 1} \in [L]^N$, containing the belief values and remaining lifetimes for the N arms.
 - 3: Initialize $\hat{W}_{N \times 1}$ to store estimated Whittle Indices.
 - 4: **for** each arm i in bandit **do**
 - 5: Let $b := \bar{b}_i, h := \bar{h}_i$ and let P be i 's transition matrix.
 - 6: Compute the myopic index Δb as:
 $\Delta b = (b P_{11}^a + (1-b) P_{01}^a) - (b P_{11}^p + (1-b) P_{01}^p)$.
 - 7: $\text{TW} \leftarrow \text{TW}(b, P)$ (Threshold Whittle Oracle).
 - 8: Set $\hat{W}_i(h, \Delta b, \text{TW})$ according to one of the interpolation functions (16) or (17).
 - 9: **end for**
 - 10: Pull the k arms with the largest values of \hat{W} .
-

which must equal the myopic index, given by Δb . The second piece is simply the horizontal line $y = \text{TW}$ that caps the function to its infinite horizon value. The linear interpolation index value is thus given by

$$\hat{W}(h, \Delta b, \text{TW}) = \min\{h \Delta b, \text{TW}\}. \quad (16)$$

The linear interpolation algorithm performs well and has very low run time, as we will demonstrate in the later sections. However, the linear interpolation can be improved by using a logistic interpolation instead. The logistic interpolation algorithm yields moderately higher rewards in many cases for a small additional compute time. For the logistic interpolation, we let

$$\hat{W}(h, \Delta b, \text{TW}) = \frac{C_1}{1 + e^{-C_2 h}} + C_3. \quad (17)$$

We now apply the three constraints on the Whittle Index established earlier and solve for the three unknowns $\{C_1, C_2, C_3\}$ to arrive at the logistic interpolation model. For the residual lifetimes of 0 and 1, we have that $\hat{W}(0) = 0$ and $\hat{W}(1) = \Delta b$. As the horizon becomes infinity, $\hat{W}(\cdot)$ must converge to TW , giving the final constraint $\hat{W}(\infty) = \text{TW}$. Solving this system yields the solution:

$$C_1 = 2\text{TW}, \quad C_2 = -\log \left(\left(\frac{\Delta b}{C_1} + \frac{1}{2} \right)^{-1} - 1 \right), \quad C_3 = -\text{TW}.$$

We note that both interpolations start from $\hat{W} = 0$ for $h = 0$ and saturate to $\hat{W} = \text{TW}$ as the horizon tends to infinity.

4.4 ANALYSIS

We start by comparing the index values computed by our interpolation algorithms with the solution by Qian et al.

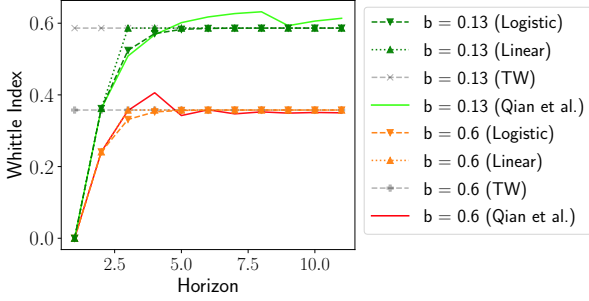


Figure 1: Whittle Indices for two belief values as computed by different algorithms. Both our algorithms are able to capture index decay and provide good estimates.

[2016]. Figure 1 shows an illustrative example, plotting the index values as a function of the residual lifetime for two belief states of an arm with the transition matrix $P_{ss'}^p = \begin{bmatrix} 0.94 & 0.06 \\ 0.54 & 0.46 \end{bmatrix}$ and $P_{ss'}^a = \begin{bmatrix} 0.54 & 0.46 \\ 0.40 & 0.60 \end{bmatrix}$. As can be seen, there is considerable agreement between the interpolated index values and the indices computed by the algorithm of Qian et al. [2016]. We note that for transition matrices that satisfy the conditions for forward threshold policies to be optimal, the limits of the interpolation values and of Qian et al. [2016] are guaranteed to agree (converging to the Threshold Whittle Index, TW).

We now turn to the analysis of the computational complexity of the algorithms. We denote by \bar{X} the expected number of arms arriving each time step and \bar{L} their average expected lifetimes. The expected number of arms at any point in time is then $\mathcal{O}(\bar{X}\bar{L})$ [Little, 1961]. Our algorithms (both versions) require a per-period cost of $\mathcal{O}(\bar{X} * |\mathcal{B}_i|) = \bar{X} * 2\bar{L}$ for the Threshold Whittle pre-computations, plus $\mathcal{O}(\bar{X})$ computations for the myopic cost, plus $\mathcal{O}(\bar{X}\bar{L} * \bar{L})$ calculations (for $\bar{X}\bar{L}$ arms, each requiring up to \bar{L} additions or multiplications) and $\mathcal{O}(\bar{X}\bar{L})$ for determining the top k indices. The overall per-period complexity of our algorithm is thus $\mathcal{O}(\bar{X}\bar{L}^2)$.

For comparison, Threshold Whittle, has per-period time complexity of $\mathcal{O}(\bar{X}\bar{L})$. The interpolation algorithm thus increases the complexity by a factor of \bar{L} . This is an acceptable trade-off when \bar{L} is low, as is typically the case in our applications, since the difference in performance is significant. Qian et al. [2016] has a per-period complexity of $\approx \mathcal{O}(\bar{X}\bar{L}^{3+\frac{1}{18}} \log(\frac{1}{\epsilon}))$, where $\log(\frac{1}{\epsilon})$ is due to a bifurcation method for approximating the Whittle index to within error ϵ on each arm and $\bar{L}^{2+\frac{1}{18}}$ is due to the best-known complexity of solving a linear program with \bar{L} variables [Jiang et al., 2020].

5 EXPERIMENTAL EVALUATION

We evaluate the performance and runtime of our proposed algorithms against several baselines. Labels marked **Logistic**

and **Linear** are our proposed algorithms. Our main baselines are: (1) a slow, but precise algorithm by **Qian et al. [2016]**, which accounts for the residual lifetime by solving the POMDP on each of the N arms and finds the k best arms to pull and (2) Threshold-Whittle algorithm [Mate et al., 2020] (marked as **TW**), which is a much faster algorithm, but rides on the assumption of a long residual time horizon. **Myopic** policy is a popularly used baseline [Mate et al., 2020, Qian et al., 2016] that plans interventions to optimize for the expected reward of the immediate next time step. **Random** is a naive baseline that pulls k arms at random. We use a real-world data set obtained from Killian et al. [2019] consisting of daily adherence data of tuberculosis patients in Mumbai, India following a prescribed treatment regimen for six months. Because the data set consists of only daily adherence records and does not contain intervention information, we use the same data imputation steps as adopted by Mate et al. [2020] to estimate the transition matrices, $P_{ss'}^a$ and $P_{ss'}^p$ for each patient empirically. We sample transition matrices from this real-world patient distribution and run simulations over a simulation length much longer than the lifetimes of the patients in the simulation. The different experimental settings are described in the following sections.

The results show the excess average intervention benefit over a ‘do-nothing’ policy, measuring the sum of rewards over all arms and all timesteps minus the reward of a policy that never pulls any arms and are normalized to set Qian et al. [2016] equal to 100%. Intervention benefit for an algorithm can thus be defined as: $\frac{100 \times (\bar{R}^{\text{ALG}} - \bar{R}^{\text{No intervention}})}{\bar{R}^{\text{Qian et al.}} - \bar{R}^{\text{No intervention}}}$ where \bar{R} is the average reward of the algorithm.

In the following subsections, we first demonstrate the dramatic speed up in planning achieved by our algorithms over Qian et al. without having to sacrifice on performance. Further, we present extensive analyses showing that the strong performance remains intact even under different conditions characterized by synchronous/asynchronous All simulation results are measured and averaged over 50 independent trials. The lower and upper error bars mark the 25th and 75th percentiles respectively. arrivals or different arrival processes for varying lifetimes of arms.

5.1 RUN TIME EVALUATION

We start by analyzing the runtimes of our algorithms in comparison to existing approaches. Figure 2 (left) compares the runtimes of our algorithms with the algorithm of Qian et al. [2016] and Mate et al. [2020]. We model the incoming stream as a Poisson process with mean daily arrivals, \bar{X} and measure the runtime as a function of \bar{X} . The lifetime of each arm, L is fixed to 5 and the number of resources is set such that $k = 10\% \times (\bar{X}L)$. For an arrival rate, \bar{X} , the simulations were run for a total length T , such that $\bar{X}T = 5000$ is the expected total arms entering the simulation. We measure

runtime as the time required for simulating $L = 5$ days in the simulation and average over 50 independent trials. As can be seen, the runtime of Qian et al. [2016] quickly far exceeds that of any of the other algorithms. Figure 2(right) offers a zoomed-in view of the fast algorithms, showing the runtime of the linear and logistic interpolation algorithms is virtually same as the runtime of the plain threshold Whittle algorithm — showing that all grow linearly in the number of arms with only marginal differences in growth rates. Simultaneously, Figure 3 plots the performance of these algorithms, measured as intervention benefit, on the y-axis. It reveals that the performance of the Linear and Logistic interpolation algorithms is at par with Qian et al. despite the dramatic speedup achieved, in the backdrop of Threshold Whittle, which suffers a severe decline in its performance.

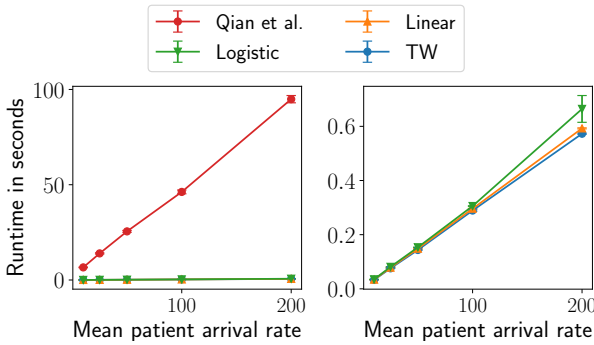


Figure 2: Linear and Logistic interpolation algorithms are nearly $150\times$ faster than Qian et al.(left). The distinction between the runtimes of TW, Linear and Logistic interpolation algorithms is shown in the zoomed in figure on the right.

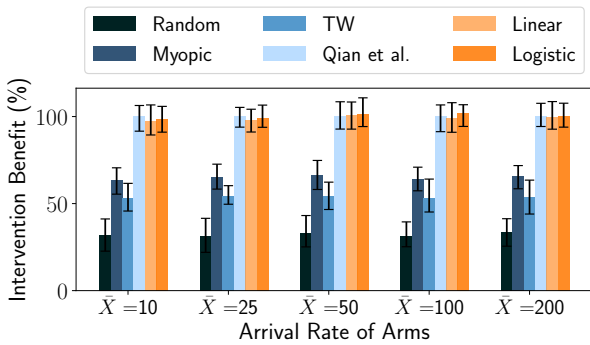


Figure 3: Intervention benefit of Linear and Logistic approximation remains high for varying sizes of patient cohorts.

5.2 FINITE HORIZON BANDITS

We now turn to analyzing the performance of the algorithms under varying lifetimes of incoming processes. We start by considering a simple S-RMAB with synchronous arms that all enter and leave the system at the same time, i.e. a ‘classic’ finite horizon RMAB. All arms arrive in the

system in the first period, thus, $X(1) = N$ and 0 otherwise, and have the same finite lifetime $L_i = L \forall i$, hence they leave the system at the same time, thus we have $Y(L+1) = N$ and 0 otherwise. In Figure 4, we vary L on the x-axis, keeping the patient cohort size constant at $N = 2000$ and the intervention resources at $k = 200$ per period. Figure 4 shows that Threshold Whittle, which assumes an infinite horizon setting, suffers from performance degradation as the planning horizon becomes short.

Intuitively, since index decay only matters for short residual lifetimes, shorter-lived arms spend a relatively higher proportion of their lifetime in the decayed state, thus exacerbating the approximation error resulting from using Threshold Whittle indices. Our interpolation algorithms yield virtually identical rewards as the exact algorithm by Qian et al. [2016] (in some cases even slightly higher ones, e.g. for $L = 10$) and do not suffer from performance degradation as the lifetime decreases. As seen before, they also yield dramatic runtime improvements, since they only use the cheaply available Myopic and Threshold Whittle indices. This result shows that it is possible to account for index decay without having to explicitly solve the costly finite horizon problem. Since the index decay phenomenon is specific to individual arms, the result further generalizes to streaming bandits, as we will see in the following section.

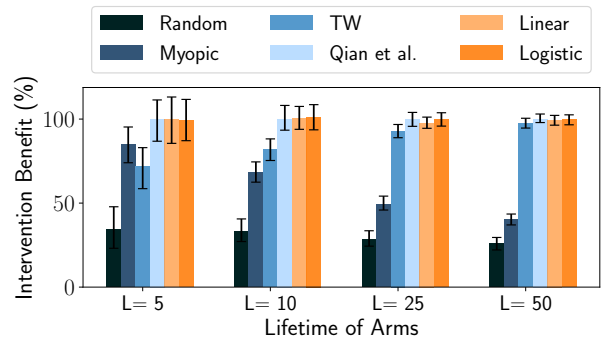


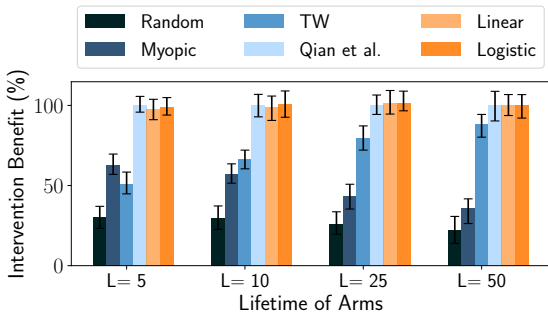
Figure 4: Performance of Threshold Whittle algorithm degrades when the lifetime of arms gets short, even when all arms start synchronously.

5.3 STREAMING BANDITS

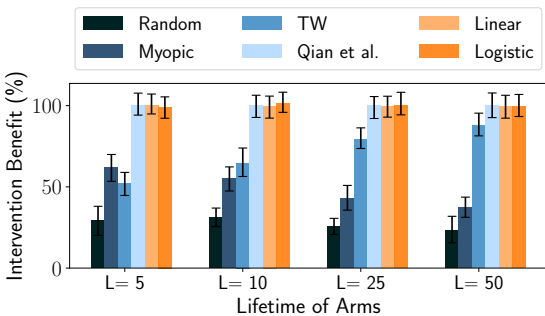
We now consider the more general S-RMAB settings where arms continuously enter and leave the system according to either a deterministic or a random schedule. The degradation in performance of Threshold Whittle indices only exacerbates in this setting, since only a fraction of the population is affected by the index decay phenomenon at any time step. This means that algorithms that are able to correctly account for index decay have more opportunities to pull arms with higher expected rewards in such settings (as opposed to a synchronous setting, where all arms decay simultaneously).

In the deterministic setting, each day, \bar{X} arms with the same lifetime L arrive, throughout the simulation. Thus, $\forall t \in [T]$, $X(t) = \bar{X}$. The population thus grows at rate \bar{X} to a size $\bar{X}L$ for the first L timesteps, then stays constant for the remaining $T - L$ time steps. In Figure 5a, we adjust \bar{X} so as to keep $\bar{X}L = 300$ for different values of L on the x-axis. We fix the number of intervention resources $k = 30$ to reflect a low-resource regime in which only 10% of the arms can be pulled. The performance of Threshold Whittle again dwindles as the lifetimes become shorter, dropping even lower than the synchronous arrivals case. The Linear and Logistic interpolation algorithms, on the other hand, remain indistinguishable in performance from Qian et al. [2016].

In the random setting, we assume arms arrive as a Poisson process with parameter \bar{X} capturing the arrival rate and depart after a fixed lifetime L . Thus $X(t) \sim \text{Poisson}(\bar{X})$ and the average number of arms in the simulation, for a sufficiently long simulation length, can be estimated as $\bar{X}L$. In Figure 5b, we again vary L on the x-axis and tune \bar{X} so as to keep fixed $\bar{X}L = 300$ and also set $k = 30$. Again, the performance of our algorithms is virtually indistinguishable, again at a fraction of the runtime cost.



(a) S-RMAB with deterministic stream.



(b) S-RMAB with stochastic stream.

Figure 5: Intervention benefit vs lifetime of an arm. Threshold Whittle drops sharply as lifetime gets shorter. Linear and Logistic interpolation remains robust to this.

5.4 SYNTHETIC DOMAINS

We perform several robustness checks using synthetic data to vary important problem parameters. The relevant figures

are provided in Appendix A. In Figure 6, we vary the proportion of forward threshold optimal patients in the population by employing rejection sampling on the tuberculosis patient data set. Although Threshold Whittle, which our interpolation relies on, is guaranteed to be asymptotically optimal only for forward threshold optimal patients, Figure 6 reveals that our algorithm works well even patients are not forward threshold optimal.

In Figure 7 we consider a patient cohort characterized by self-correcting and non-recoverable patients, consistent with [Mate et al., 2020]. Self-correcting patients display a tendency to “correct” themselves switching from the bad state to the good state irrespective of the action taken, whereas non-recoverable patients don’t do so even upon intervening. It is shown that under such situations, Threshold Whittle, that plans for long term reward, focuses exclusively on the non-recoverable patients. However, when the residual lifetime is rather short, Threshold Whittle stands at a disadvantage and its performance accordingly dwindles in the presence of non-recoverable patients as shown in Figure 7.

Finally, in Figure 8 we test the robustness of our algorithms in different scenarios with varying levels of resource availability and corroborate that the performance of our algorithms remains consistent. The run time of our algorithms remains consistently low across all specifications.

6 CONCLUSION

We study *streaming bandits*, or S-RMAB, a class of bandits where heterogeneous arms arrive and leave asynchronously under possibly random streams. While efficient RMAB algorithms for computing Whittle Indices for infinite horizon settings exist, for the finite horizon settings however, these algorithms are either comparatively costly or not suitable for estimating the Whittle Indices accurately. To tackle this, we provide a new scalable approach that allows for efficient computation of the Whittle Index values for finite horizon restless bandits while also adapting to more general S-RMAB settings. Our approach leverages a phenomenon called *index decay* to compute the indices for each arm. Through an extensive set of experiments on real-world and synthetic data, we demonstrate that our approach provides good estimates of Whittle Indices, and yield over $150\times$ runtime improvements without loss in performance.

Future Directions: Streaming bandits as a problem class are highly relevant for modelling problems in the healthcare and social work domains, but potential application areas abound, including sustainability, conservation, maintenance, finance and many others. We have provided algorithms that scale to relevant problem sizes, making this problem class accessible to real-world applications. Regarding methodological expansions, future work could focus on planning frameworks that leverage human-in-the-loop approaches.

References

- N. Akbarzadeh and A. Mahajan. Restless bandits with controlled restarts: Indexability and computation of Whittle index. In *2019 IEEE Conference on Decision and Control*. IEEE, 2019.
- Biswarup Bhattacharya. Restless bandits visiting villages: A preliminary study on distributing public health services. In *Proceedings of the 1st ACM SIGCAS Conference on Computing and Sustainable Societies*, pages 1–8, 2018.
- Arpita Biswas, Shweta Jain, Debmalya Mandal, and Y Narahari. A truthful budget feasible multi-armed bandit mechanism for crowdsourcing time critical tasks. In *Proceedings of the 2015 International Conference on Autonomous Agents and Multiagent Systems*, pages 1101–1109, 2015.
- J Nell Brownstein, Farah M Chowdhury, Susan L Norris, Tanya Horsley, Leonard Jack Jr, Xuanping Zhang, and Dawn Satterfield. Effectiveness of community health workers in the care of people with hypertension. *American journal of preventive medicine*, 32(5):435–447, 2007.
- Alicia H Chang, Andrea Polesky, and Gulshan Bhatia. House calls by community health workers and public health nurses to improve adherence to isoniazid monotherapy for latent tuberculosis infection: a retrospective study. *BMC public health*, 13(1):894, 2013.
- K.D. Glazebrook, D. Ruiz-Hernandez, and C. Kirkbride. Some indexable families of restless bandit problems. *Adv. Appl. Probab*, pages 643–672, 2006.
- Jeffrey Thomas Hawkins. *A Lagrangian decomposition approach to weakly coupled dynamic optimization problems and its applications*. PhD thesis, Massachusetts Institute of Technology, 2003.
- Y. Hsu. Age of information: Whittle index for scheduling stochastic arrivals. In *2018 IEEE International Symposium on Information Theory*. IEEE, 2018.
- Weici Hu and Peter Frazier. An asymptotically optimal index policy for finite-horizon restless bandits. *arXiv preprint arXiv:1707.00205*, 2017.
- S. Jiang, Z. Song, O. Weinstein, and H. Zhang. Faster dynamic matrix inverse for faster Ips. *arXiv preprint arXiv:2004.07470*, 2020.
- Varun Kanade, H Brendan McMahan, and Brent Bryan. Sleeping experts and bandits with stochastic action availability and adversarial rewards. In *Artificial Intelligence and Statistics*, pages 272–279. PMLR, 2009.
- J. A. Killian, B. Wilder, A. Sharma, V. Choudhary, B. Dilkina, and M. Tambe. Learning to prescribe interventions for tuberculosis patients using digital adherence data. In *KDD*, 2019.
- Robert Kleinberg, Alexandru Niculescu-Mizil, and Yogeshwer Sharma. Regret bounds for sleeping experts and bandits. *Machine learning*, 80(2):245–272, 2010.
- Jerome Le Ny, Munther Dahleh, and Eric Feron. Multi-uav dynamic routing with partial observations using restless bandit allocation indices. In *2008 American Control Conference*, pages 4220–4225. IEEE, 2008.
- Elliot Lee, Mariel S Lavieri, and Michael Volk. Optimal screening for hepatocellular carcinoma: A restless bandit model. *Manufacturing & Service Operations Management*, 21(1):198–212, 2019.
- John DC Little. A proof for the queuing formula: $L = \lambda w$. *Operations research*, 9(3):383–387, 1961.
- K. Liu and Q. Zhao. Indexability of restless bandit problems and optimality of Whittle index for dynamic multichannel access. *IEEE Transactions on Information Theory*, pages 5547–5567, 2010a.
- K. Liu and Q. Zhao. Indexability of restless bandit problems and optimality of Whittle index for dynamic multichannel access. *IEEE Transactions on Information Theory*, 56(11):5547–5567, 2010b.
- Bernd Löwe, Jürgen Unützer, Christopher M Callahan, Anthony J Perkins, and Kurt Kroenke. Monitoring depression treatment outcomes with the patient health questionnaire-9. *Medical care*, pages 1194–1201, 2004.
- Aditya Mate, Jackson A Killian, Haifeng Xu, Andrew Perrault, and Milind Tambe. Collapsing bandits and their application to public health interventions. In *Advances in Neural and Information Processing Systems (NeurIPS)*, 2020.
- Nicolas Meuleau, Milos Hauskrecht, Kee-Eung Kim, Leonid Peshkin, Leslie Pack Kaelbling, Thomas L Dean, and Craig Boutilier. Solving very large weakly coupled Markov decision processes. In *AAAI/IAAI*, pages 165–172, 1998.
- Christopher Mundorf, Arti Shankar, Tracy Moran, Sherry Heller, Anna Hassan, Emily Harville, and Maureen Lichtveld. Reducing the risk of postpartum depression in a low-income community through a community health worker intervention. *Maternal and child health journal*, 22(4):520–528, 2018.
- Patrick M Newman, Molly F Franke, Jafet Arrieta, Hector Carrasco, Patrick Elliott, Hugo Flores, Alexandra Friedman, Sophia Graham, Luis Martinez, Lindsay Palazuelos, et al. Community health workers improve disease control and medication adherence among patients with diabetes and/or hypertension in Chiapas, Mexico: an observational stepped-wedge study. *BMJ Global Health*, 2018.

- José Nino-Mora. Computing a classic index for finite-horizon bandits. *INFORMS Journal on Computing*, 23(2):254–267, 2011.
- Christos H Papadimitriou and John N Tsitsiklis. The complexity of optimal queueing network control. In *Proceedings of IEEE 9th Annual Conference on Structure in Complexity Theory*, pages 318–322. IEEE, 1994.
- Y. Qian, C. Zhang, B. Krishnamachari, and M. Tambe. Restless poachers: Handling exploration-exploitation trade-offs in security domains. In *AAMAS*, 2016.
- Jane Rahedi Ong’ang’o, Christina Mwachari, Hillary Kipruto, and Simon Karanja. The effects on tuberculosis treatment adherence from utilising community health workers: a comparison of selected rural and urban settings in kenya. *PLoS One*, 9(2):e88937, 2014.
- B. Sombabu, A. Mate, D. Manjunath, and S. Moharir. Whittle index for aoi-aware scheduling. In *IEEE International Conference on Communication Systems & Networks (COMSNETS)*. IEEE, 2020.
- P. Whittle. Restless bandits: Activity allocation in a changing world. *J. Appl. Probab.*, 25(A):287–298, 1988.
- Gabriel Zayas-Caban, Stefanus Jasin, and Guihua Wang. An asymptotically optimal heuristic for general nonstationary finite-horizon restless multi-armed, multi-action bandits. *Advances in Applied Probability*, 51(3):745–772, 2019.

A ROBUSTNESS CHECKS

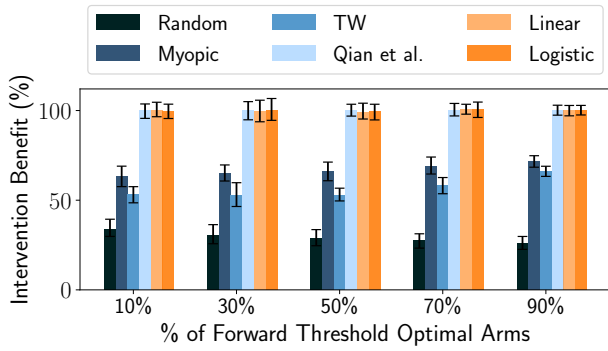


Figure 6: Performance of our algorithm remains robust even when population is composed of a varying fraction of forward threshold optimal arms

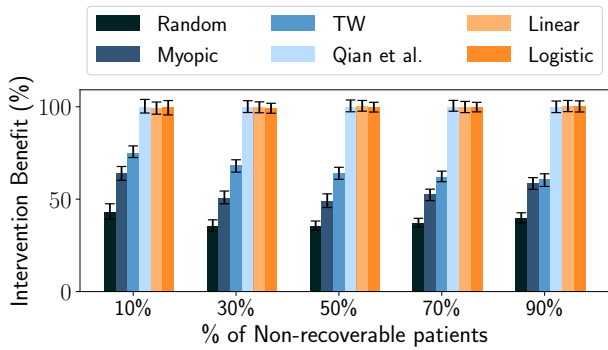


Figure 7: Performance of Threshold Whittle begins to dwindle when the fraction of non-recoverable patients in the cohort increases, but our interpolation algorithms remain robust

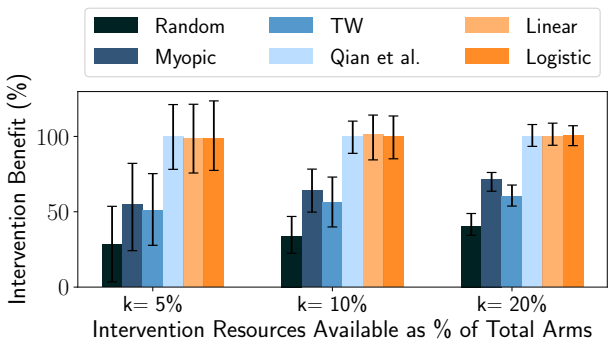


Figure 8: Performance of our algorithm remains robust under varying levels of available resources